Resonant grazing bifurcations in simple impacting systems

Indranil Ghosh and David J.W. Simpson

School of Mathematical and Computational Sciences
Massey University, Palmerston North, New Zealand

December 18, 2024

Impact Oscillators

- Many engineering systems involve vibrations and impacts, e.g. impact print hammers, gear assemblies, machinery for milling, bells, and shock absorbers.

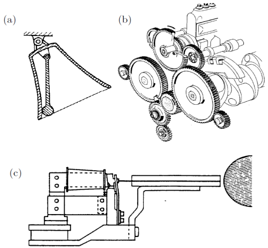

Figure: Examples of simple impacting systems: (a) a bell, (b) a gear assembly, (c) an impact print hammer. Picture taken from *di Bernardo, Champneys, Budd, Kowalczyk, 2008*.

The impact oscillator model

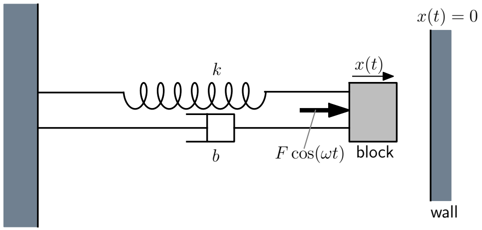

Figure: A hard-impact oscillator model: $\ddot{x} + b\dot{x} + x + 1 = F\cos(\omega t)$ and $\dot{x} \mapsto -r\dot{x}$ whenever $x = 0$.

The impact oscillator model

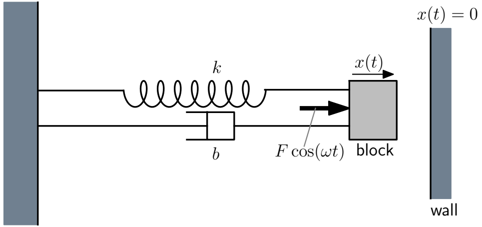

Figure: A hard-impact oscillator model: $\ddot{x} + b\dot{x} + x + 1 = F\cos(\omega t)$ and $\dot{x} \mapsto -r\dot{x}$ whenever $x = 0$.

- If the block hits the wall with zero velocity, this is a *grazing* impact.
- A grazing bifurcation occurs when the limit cycle has a grazing impact.

Literature Survey

- S.W. Shaw, *J. Appl. Mech.*, 1985.
- S.W. Shaw and P.J. Holmes, *J. Sound Vib.*, 1983.
- J. de Weger *et al.*, *Phys. Rev. Lett.*, 1996.
- P. T. Piiroinen *et al.*, *J. Nonlinear Sci.*, 2004.
- J. Qiu and Z.C. Feng, *Computers & Structures*, 2000.
- T. Witelski *et al.*, *J. Sound Vib.*, 2014.
- S. Banerjee *et al.*, *Phys. Rev. E*, 2009.
- J. Molenaar *et al.*, *Nonlinearity*, 2001.
- E. Pavlovskaia *et al.*, *Int. J. Bifurcation Chaos*, 2010.

Experimental example

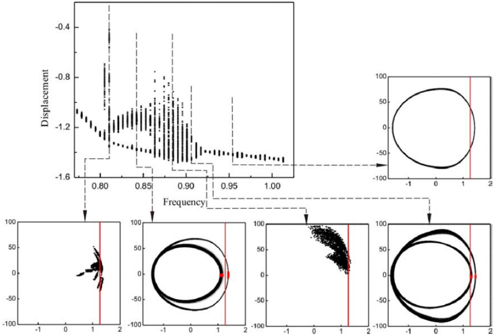

Figure: Bifurcation diagram obtained from the paper by Pavlovskaia *et al.*, Int. J. Bifurcation Chaos, 2010.

Experimental example

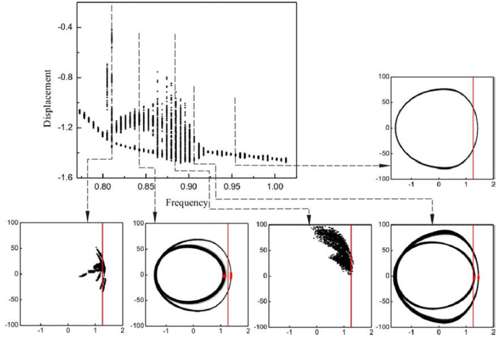

Figure: Bifurcation diagram obtained from the paper by Pavlovskaia *et al.*, Int. J. Bifurcation Chaos, 2010.

- Why does a stable period-two solution appear so close to grazing?

Model

- The nondimensionalised equations of our oscillator model are given by

$$\dot{x} = y,$$
$$\dot{y} = F\cos(\omega t) - by - x - 1,$$

where $x(t)$ and $y(t)$ are the displacement and the velocity of the oscillator with the damping ratio $b > 0$.

Model

- The nondimensionalised equations of our oscillator model are given by

$$\dot{x} = y,$$
$$\dot{y} = F\cos(\omega t) - by - x - 1,$$

where $x(t)$ and $y(t)$ are the displacement and the velocity of the oscillator with the damping ratio $b > 0$.

- We treat F as the primary bifurcation parameter.

Model

- The nondimensionalised equations of our oscillator model are given by

$$\begin{aligned}\dot{x} &= y,\\ \dot{y} &= F\cos(\omega t) - by - x - 1,\end{aligned}$$

  where $x(t)$ and $y(t)$ are the displacement and the velocity of the oscillator with the damping ratio $b > 0$.
- We treat F as the primary bifurcation parameter.
- The values of F and t that occur at grazing are implicitly given by

$$\begin{aligned}t_{\text{graz}} &= \frac{1}{\omega}\tan^{-1}\left(\frac{b\omega}{1-\omega^2}\right),\\ F_{\text{graz}}^2 &= (1-\omega^2)^2 + b^2\omega^2.\end{aligned}$$

Typical phase portrait

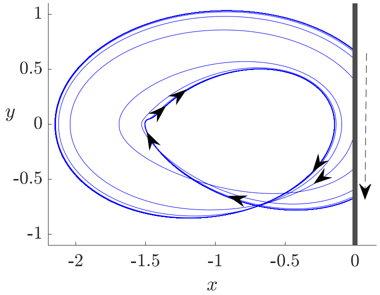

Figure: A typical phase portrait of the impact oscillator.

Bifurcation diagram

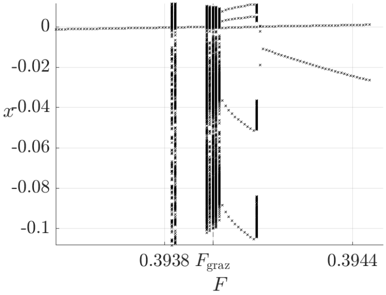

Figure: A typical bifurcation diagram of the impact oscillator.

Poincaré map

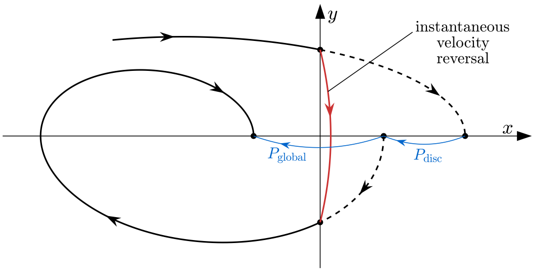

Figure: An illustration of the Poincaré map.

Poincaré map

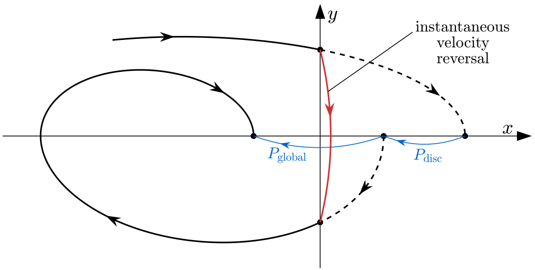

Figure: An illustration of the Poincaré map.

- We use $y = 0$ as the Poincaré section. The map is given by $(x', z') = P(x, z)$ where $z = t - t_{\text{graz}} \mod \frac{2\pi}{\omega}$.
- We evaluate P numerically, using an explicit formula for the flow, and event detection for determining where orbits return to the Poincaré section.

Poincaré map

- The map P can be expressed as

$$P = P_{\text{global}} \circ P_{\text{disc}}.$$

Poincaré map

- The map P can be expressed as

$$P = P_{\text{global}} \circ P_{\text{disc}}.$$

- Here

$$P_{\text{disc}}(x, z; F) = \begin{cases} \begin{bmatrix} x \\ z \end{bmatrix}, & x \leq 0, \\ \begin{bmatrix} r^2 x + \tilde{O}(3) \\ z - \frac{\sqrt{2}}{\omega}(1+r)\sqrt{x} + \tilde{O}(2) \end{bmatrix}, & x > 0. \end{cases}$$

Poincaré map

- To first order, the Taylor expansion of P_{global} about $(x, z; F) = (0, 0; F_{\text{graz}})$ can be written as

$$P_{\text{global}} = K \begin{bmatrix} x \\ z \end{bmatrix} + \frac{F - F_{\text{graz}}}{F_{\text{graz}}} \begin{bmatrix} 1 - a_{11} \\ -a_{21} \end{bmatrix} + O(2),$$

where

$$K = \begin{bmatrix} a_{11} & \omega^2 a_{12} \\ \frac{a_{21}}{\omega^2} & a_{22} \end{bmatrix},$$

and each a_{ij} is the (i, j) entry of

$$A = \exp\left(\frac{2\pi}{\omega} \begin{bmatrix} 0 & 1 \\ -1 & -b \end{bmatrix} \right).$$

Poincaré map

- Note that

$$a_{11} = \frac{\lambda_1 e^{\frac{2\pi}{\omega}\lambda_2} - \lambda_2 e^{\frac{2\pi}{\omega}\lambda_2}}{\lambda_1 - \lambda_2}, \qquad a_{12} = \frac{e^{\frac{2\pi}{\omega}\lambda_1} - e^{\frac{2\pi}{\omega}\lambda_2}}{\lambda_1 - \lambda_2},$$

$$a_{21} = -a_{12}, \qquad a_{22} = \frac{(\lambda_1 + b)e^{\frac{2\pi}{\omega}\lambda_2} - (\lambda_2 + b)e^{\frac{2\pi}{\omega}\lambda_1}}{\lambda_1 - \lambda_2},$$

where K has eigenvalues $\lambda_{1,2} = \alpha \pm i\beta$.

Poincaré map

- Note that

$$a_{11} = \frac{\lambda_1 e^{\frac{2\pi}{\omega}\lambda_2} - \lambda_2 e^{\frac{2\pi}{\omega}\lambda_2}}{\lambda_1 - \lambda_2}, \qquad a_{12} = \frac{e^{\frac{2\pi}{\omega}\lambda_1} - e^{\frac{2\pi}{\omega}\lambda_2}}{\lambda_1 - \lambda_2},$$

$$a_{21} = -a_{12}, \qquad a_{22} = \frac{(\lambda_1 + b)e^{\frac{2\pi}{\omega}\lambda_2} - (\lambda_2 + b)e^{\frac{2\pi}{\omega}\lambda_1}}{\lambda_1 - \lambda_2},$$

  where K has eigenvalues $\lambda_{1,2} = \alpha \pm i\beta$.
- Here,

$$\alpha = -\frac{b}{2}, \qquad \beta = \sqrt{1 - \frac{b^2}{4}}.$$

Poincaré map

- Note that

$$a_{11} = \frac{\lambda_1 e^{\frac{2\pi}{\omega}\lambda_2} - \lambda_2 e^{\frac{2\pi}{\omega}\lambda_2}}{\lambda_1 - \lambda_2}, \qquad a_{12} = \frac{e^{\frac{2\pi}{\omega}\lambda_1} - e^{\frac{2\pi}{\omega}\lambda_2}}{\lambda_1 - \lambda_2},$$

$$a_{21} = -a_{12}, \qquad a_{22} = \frac{(\lambda_1 + b)e^{\frac{2\pi}{\omega}\lambda_2} - (\lambda_2 + b)e^{\frac{2\pi}{\omega}\lambda_1}}{\lambda_1 - \lambda_2},$$

  where K has eigenvalues $\lambda_{1,2} = \alpha \pm i\beta$.
- Here,

$$\alpha = -\frac{b}{2}, \qquad \beta = \sqrt{1 - \frac{b^2}{4}}.$$

- Also K has trace $\tau = 2e^{\frac{2\pi\alpha}{\omega}} \cos\left(\frac{2\pi\beta}{\omega}\right)$ and determinant $\delta = e^{\frac{4\pi\alpha}{\omega}}$.

Numerics

- For a period-p solution of our map P with one point in $x > 0$, this point is a fixed point of $P^p_{\mathrm{global}} \circ P_{\mathrm{disc},R}$.

Numerics

- For a period-p solution of our map P with one point in $x > 0$, this point is a fixed point of $P^p_{\rm global} \circ P_{{\rm disc},R}$.
- *Maximal* periodic solutions are those with exactly one point in $x > 0$ (such periodic solutions are the most likely to be stable because the square-root singularity is highly destabilising)

Numerics

- For a period-p solution of our map P with one point in $x > 0$, this point is a fixed point of $P_{\text{global}}^p \circ P_{\text{disc},R}$.
- *Maximal* periodic solutions are those with exactly one point in $x > 0$ (such periodic solutions are the most likely to be stable because the square-root singularity is highly destabilising)
- Since $P_{\text{global}}^p \circ P_{\text{disc},R}$ is smooth, standard numerical methods like Newton's method can be used to follow fixed points while $x > 0$.

Numerics

- For a period-p solution of our map P with one point in $x > 0$, this point is a fixed point of $P_{\text{global}}^{p} \circ P_{\text{disc},R}$.
- *Maximal* periodic solutions are those with exactly one point in $x > 0$ (such periodic solutions are the most likely to be stable because the square-root singularity is highly destabilising)
- Since $P_{\text{global}}^{p} \circ P_{\text{disc},R}$ is smooth, standard numerical methods like Newton's method can be used to follow fixed points while $x > 0$.
- That is, given a guess for (x_0, z_0), we compute (y_1, z_1), (y_2, z_2), and (x_3, z_3), and $(x_4, z_4) = P_{\text{global}}^{p}(x_3, z_3; F)$. Then let $G(x_0, z_0; F) = (x_4, z_4) - (x_0, z_0)$ and continue zeros of G.

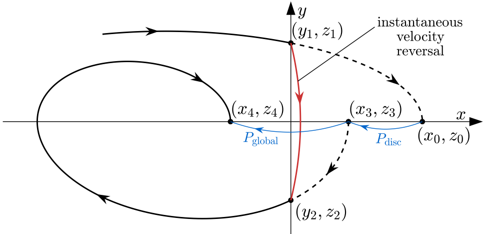

Numerics

- However, Newton's method fails near grazing because $P_{\text{disc},R}$ contains $\sqrt{x}$ (if $x < 0$, the method blows up!).

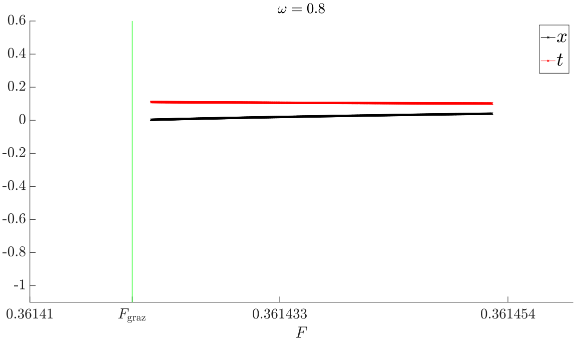

Numerics

- However, Newton's method fails near grazing because $P_{\mathrm{disc},R}$ contains $\sqrt{x}$ (if $x < 0$, the method blows up!).

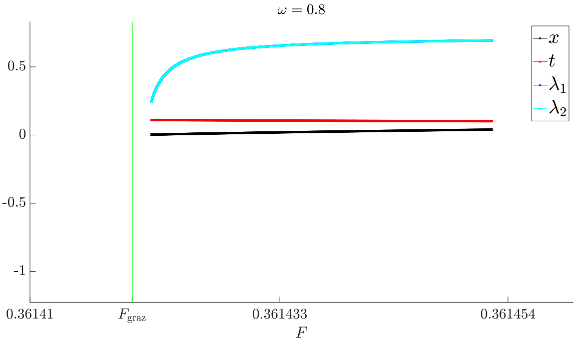

Numerics

- So instead we guess (y_1, z_1), then compute (x_0, z_0), (y_2, z_2), and (x_3, z_3), and $(x_4, z_4) = P^p_{\text{global}}(x_3, z_3; F)$. Then let $V(y_1, z_1; F) = (x_4, z_4) - (x_0, z_0)$.

Numerics

- So instead we guess (y_1, z_1), then compute (x_0, z_0), (y_2, z_2), and (x_3, z_3), and $(x_4, z_4) = P^p_{\text{global}}(x_3, z_3; F)$. Then let $V(y_1, z_1; F) = (x_4, z_4) - (x_0, z_0)$.
- The function V maps the impact velocity and z-value to the variation (or change) in displacement and z-value.

Numerics

- So instead we guess (y_1, z_1), then compute (x_0, z_0), (y_2, z_2), and (x_3, z_3), and $(x_4, z_4) = P^p_{\text{global}}(x_3, z_3; F)$. Then let $V(y_1, z_1; F) = (x_4, z_4) - (x_0, z_0)$.
- The function V maps the impact velocity and z-value to the variation (or change) in displacement and z-value.
- We call the function V as the VIVID function that follows the zeros of a function mapping **V**elocity **I**nto **V**ariation **I**n **D**isplacement.

One-parameter bifurcation diagram

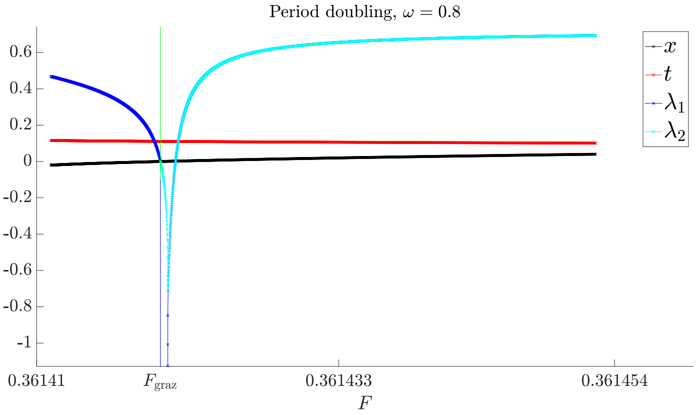

One-parameter bifurcation diagram

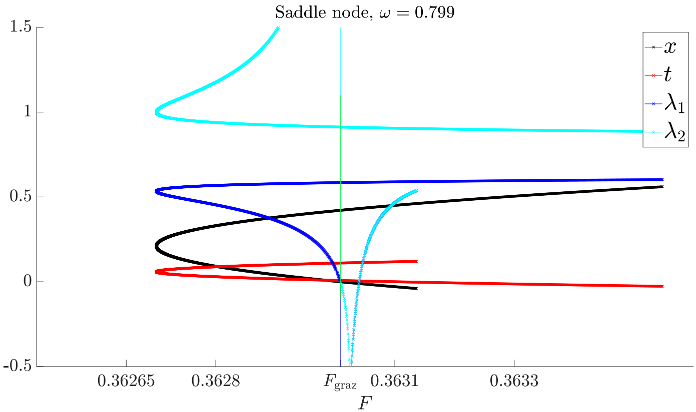

Two-parameter bifurcation diagram

- We are able to compute the two-parameter bifurcation diagram because of our new numerical tool.

Two-parameter bifurcation diagram

- We are able to compute the two-parameter bifurcation diagram because of our new numerical tool.
- The location of the codimension-two point is understood.

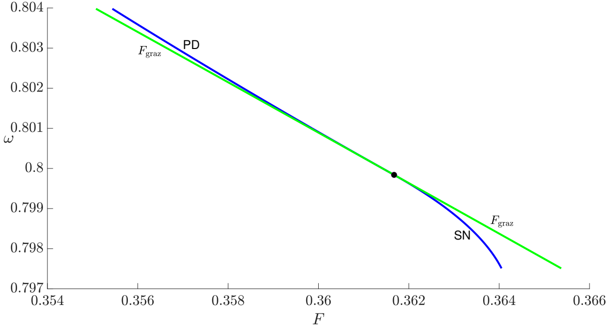

Resonance

- Branches of maximal periodic solutions emanate from the grazing bifurcation, either to the left or the right, and Nordmark (*Nonlinearity*, 2001) showed that this is determined by the values of τ and δ.

Resonance

- Branches of maximal periodic solutions emanate from the grazing bifurcation, either to the left or the right, and Nordmark (*Nonlinearity*, 2001) showed that this is determined by the values of τ and δ.

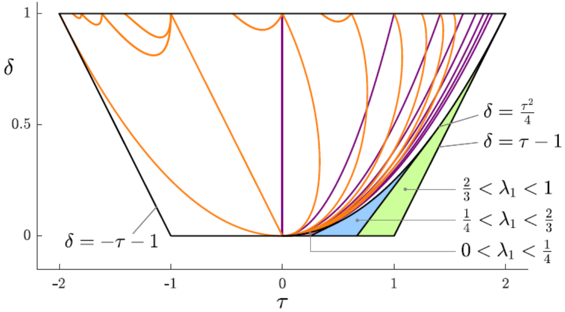

-

Figure: Division of the (τ, δ) plane.

Resonance

- The eigenvalues of K are complex, and thus can be written as $\lambda_{1,2} = r\exp(\pm i\theta)$, where $r > 0$ and $0 < \theta < \pi$.

Resonance

- The eigenvalues of K are complex, and thus can be written as $\lambda_{1,2} = r\exp(\pm i\theta)$, where $r > 0$ and $0 < \theta < \pi$.
- Thus, we have $\tau = 2r\cos(\theta)$ and $\delta = r^2$.

Resonance

- The eigenvalues of K are complex, and thus can be written as $\lambda_{1,2} = r\exp(\pm i\theta)$, where $r > 0$ and $0 < \theta < \pi$.
- Thus, we have $\tau = 2r\cos(\theta)$ and $\delta = r^2$.
- The period-p solution changes from emanating to the left to emanating to the right when $\sin(p\theta) = 0$.

Resonance

- The eigenvalues of K are complex, and thus can be written as $\lambda_{1,2} = r\exp(\pm i\theta)$, where $r > 0$ and $0 < \theta < \pi$.
- Thus, we have $\tau = 2r\cos(\theta)$ and $\delta = r^2$.
- The period-p solution changes from emanating to the left to emanating to the right when $\sin(p\theta) = 0$.
- In particular with $p = 2$ this is $\tau = 0$, which corresponds to your codimension-two point.

Resonance

- The eigenvalues of K are complex, and thus can be written as $\lambda_{1,2} = r\exp(\pm i\theta)$, where $r > 0$ and $0 < \theta < \pi$.
- Thus, we have $\tau = 2r\cos(\theta)$ and $\delta = r^2$.
- The period-p solution changes from emanating to the left to emanating to the right when $\sin(p\theta) = 0$.
- In particular with $p = 2$ this is $\tau = 0$, which corresponds to your codimension-two point.
- Solving which we get a rational ratio of ω and β given by

$$\frac{\omega}{\beta} = \frac{4}{5}$$

corresponding to *resonance*.

Conclusion

- We have shown that the oscillator has a stable period-two solution near grazing because it is near resonance.

Conclusion

- We have shown that the oscillator has a stable period-two solution near grazing because it is near resonance.
- We have developed a new numerical tool called **VIVID** using which the issue of "numerical algorithms falling off the side of square-root near grazing" is circumvented.

Conclusion

- We have shown that the oscillator has a stable period-two solution near grazing because it is near resonance.
- We have developed a new numerical tool called **VIVID** using which the issue of "numerical algorithms falling off the side of square-root near grazing" is circumvented.
- We produce two-parameter bifurcation diagrams showing curves of saddle-node and period-doubling bifurcation emanating from a codimension-two grazing bifurcation.

Conclusion

- We have shown that the oscillator has a stable period-two solution near grazing because it is near resonance.
- We have developed a new numerical tool called **VIVID** using which the issue of "numerical algorithms falling off the side of square-root near grazing" is circumvented.
- We produce two-parameter bifurcation diagrams showing curves of saddle-node and period-doubling bifurcation emanating from a codimension-two grazing bifurcation.
- However, it remains to unfold such codimension-two points theoretically (and we have started to work on this). Hopefully, this can explain why the SN curve bends away from F_{graz} faster than the PD curve.

Acknowledgements

MARSDEN FUND
TE PŪTEA RANGAHAU A MARSDEN

ROYAL SOCIETY
TE APĀRANGI

The End

Thank you! Questions?